

An approximate analytical solution of the gear meshing problem based on MSM using DynPy Python library

Krzysztof TWARDOCH¹*, Krzysztof KACZMARZYK², Grzegorz DŁUGOPOLSKI²,
 and Bogumił CHILIŃSKI¹

¹ Division of Numerical Methods and Intelligent Structures, Faculty of Automotive and Construction Machinery Engineering,
 Warsaw University of Technology, Poland

² Faculty of Automotive and Construction Machinery Engineering, Warsaw University of Technology, Poland

Abstract. The paper presents the mathematical and numerical analysis of a 1-DOF (one-degree-of-freedom) dynamic model of the helical gear with time-varying mesh stiffness (TVMS). The article aims to determine an analytical solution for the presented model using a proprietary computational environment and to verify the results with numerical simulations and other solutions available in the literature. The paper presents the determination of a 2-DOF (two-degree-of-freedom) dynamic model and its reduction to a 1-DOF model. The concept of the created environment, the applied libraries, and the application basics are discussed. Based on the work effects, an analytical solution using the multiple scales method (MSM) was found and positively verified. The article presents the convergence of the obtained results and the added value as an analytical solution. This confirms the effectiveness of the novelty approach, which provides a framework that bridges the gap between directly determining a solution and manual calculations. It should be noted that time complexity is especially important for performance computing. Observations suggest significant advantages to using an analytical solution due to its precision and relatively low computational cost. Although obtaining an analytical solution is more time-consuming, it reduces the possibility of errors with numerical methods.

Keywords: gear meshing; parametric vibrations; time-varying mesh stiffness (TVMS); multiple scales method (MSM); analytical modeling; numerical simulations; drive system; gear dynamics.

1. INTRODUCTION

There is growing interest in sophisticated computational methods for gears commonly used in industry [1, 2]. This is related to the demand for increasingly heavy-duty constructions. This is dictated by considerations of energy savings, i.e., reducing the energy intensity of machinery and equipment. Thus, the current trend in the design of gear is characterized by a desire to minimize dimensions and weight. There is a direct proportional relationship between energy savings and design strain. This trend implies a change in the frequency structure of the system (a change in eigenfrequencies) due to a change in the basic dynamic parameters of gear such as mass and stiffness. The demand for optimization of mass is associated with an unknown impact on the dynamics of the system. Clearly, changing the parameters of the system results in a completely different dynamic response.

In connection with the outlined problem of gear design, a demand arises for precise computational methods based on the determination of analytical solutions [3–5]. Analytical methods are particularly interesting from the point of view of the opti-

mization process because they provide an explicit mathematical description of the system in the form of clear formulas. This is conducive to the creation of software implementations, enables fast calculations, and obtaining results for different input data, i.e., for different values of system parameters.

One of the important exploratory problems of gears is the possibility of parametric resonance. The main reason for the occurrence of this resonance phenomenon (parametric resonance) is the time-varying stiffness of the mesh, which is due to the essence of the operation of gears, i.e., the meshing of mating wheels and the associated periodically varying number of pairs of teeth that are in the pinion at a given time instant.

This article aims to provide advanced calculational environment and to analyze the parametric vibration of a helical gear system with time-varying mesh stiffness (TVMS) using the multiple scales method (MSM) and numerical methods within this environment. This study considered a 2-DOF model of the helical gear system. Then, it was reduced to a 1-DOF system to find an analytical solution, evaluate its adequacy, and analyze the phenomenon of parametric vibrations generated in the mesh. The 2-DOF model served as a reference model. In turn, the 1-DOF model served as the basis for determining analytical solutions.

The characteristic of a good model is conciseness (appropriate level of abstraction) and not size (over-expansion). Therefore,

*e-mail: krzysztof.twardoch@pw.edu.pl

Manuscript submitted 2025-03-24, revised 2025-08-13, initially accepted for publication 2025-09-25, published in January 2026.

one of this paper's goals is to propose a simple dynamic model of a helical gearbox and to check whether it corresponds to the physical operating parameters of such a gearbox. The intention is a qualitative analysis. The authors have assumed that considering the problem at this stage of the work will not focus on the exact selection of the system parameters and the possibility of their physical realisation. According to the concept adopted, the proposed approach allows, with the assumed error, to determine analytically the system dynamic characteristics, without knowledge of numerical data – no numerical simulations are necessary.

The following milestones were defined based on the analysis of the set work objective and the issues to be addressed:

1. Development of an environment supporting analytical calculations, providing tools to support activities at each stage of the calculations.
2. Determination of an analytical solution in the developed environment and verification with other publications.
3. Perform numerical simulations in the created environment for the normative engagement model and for the MSM to verify the effectiveness of the created framework.
4. Compare the forces for different engagement models to select the most accurate (adequate) model.

The realization of the thesis objective fills the gap between the automatic execution of calculations in CAS systems (black box model) and a full understanding of the MSM and manual execution of calculations step by step. This is the added value of the thesis and its novelty.

A comparative analysis of the analytical and numerical model was assumed to assess the proposed methodology effectiveness within the prepared framework and developed by authors' DynPy library. Based on the verified analytical solution, a series of simulations can be performed to analyze the problem under consideration thoroughly. A mathematical model is established describing the relationships between the key parameters affecting the occurrence of parametric resonance of the gearbox. The mathematical conditions for the occurrence of parametric resonance are confirmed as the solution obtained by multiple scales method (MSM).

As already noted (4th paragraph), a good model is characterised by conciseness (an appropriate level of abstraction) rather than size (excessive complexity) to capture the essence of a specific dynamic phenomenon, as exemplified by studies [6–8]. Notwithstanding that the considered model is relatively simple and current computing capabilities allow for solving more complex problems, this approach offers certain advantages, allowing for:

- Verify the correctness of the proposed solution (environment, methodology and mathematical dependencies) by analysis and comparison with publications on a similar topic, for example [6, 7, 9].
- Easier understanding of the phenomenon essence of inter-tooth dynamics – considerations focus only on meshing vibrations, such as references [8, 10].
- Complementary knowledge of the phenomena involved is essential for the efficient analysis of more complex systems, which is why this approach allows for a better understanding

of the problem under consideration, thereby enhancing our understanding of real-world systems.

Mathematical modeling has been used for many years. Various mathematical models have recently been created for numerous applications [10, 11]. The flagship research article [12] presents a classic overview of such models. This paper discusses typically used mathematical models and provides a general classification of them. The research focused on the dynamics of helical gears very often refers to the nature of their operation related to the generation of parametric vibrations associated with the time-varying number of pairs of teeth in contact, i.e., in the line-of-action. An interesting example of parametric vibrations and instabilities of an elliptical gear pair research is presented in [13]. The publication evaluates the influence of basic parameters on solution stability. The research used a model to consider factors such as eccentricity or varying mesh stiffness. These effects caused vibrations in the system, which led to the determination of different combination resonances. The calculation results show the coupling effect between the selected frequencies. The authors show that the coupling effect results from the simultaneous occurrence of load, time-varying mesh stiffness, and eccentricity. Studies comparing elliptical and circular gears have unveiled lower vibration amplitudes in elliptical gears, exploring the intricate interactions between eccentricity, stiffness, and load that lead to vibrations and instability in these gear configurations [13]. It is imperative to determine the ranges of irregular gear behaviour, as this may cause chaotic phenomena. This is demonstrated by a numerical investigation on gear dynamics [6]. It presents simulation studies based on a nonlinear mathematical model of a gear transmission that considers variable mesh stiffness and backlash, which made it possible to identify areas where the analysed system behaved chaotically. This is illustrated as a frequency spectrum, a bifurcation diagram, a Lyapunov exponent, and a Poincaré map (section).

The interesting field of investigation under the gears is its modeling and experimental testing [3–5, 7, 9, 14–16]. Noteworthy is a publication [17], where the subject of analysis was a helical gear system. A system of shafts, bearings, and disks representing gears was used for modeling. Gears are part of the parametrically excited system because of time-varying mesh stiffness. This study proposed a matrix with harmonic frequencies representing parametrically excited vibration transfer functions. The nonlinear equation of motion for gears was linearized to an equation with the excitation of harmonic frequencies. The proposed transfer matrix can easily show the contribution of the harmonic components. The research follows on from that presented in the papers [18, 19]. Article [18] presents the analysis of a simplified model. The results obtained were used to analyze gearbox vibrations under axial load. The model includes a shaft, gear system, and housing. In addition, mesh stiffness and a solution to the equation of motion were used to determine the axial force. The relationship between strain and load is used for this purpose. The noise generated by helical gears is also a problem that requires analysis. One research direction is the use of simplified systems subjected to axial load. Models consisting of shafts, bearings, and helical gears are used for this purpose [19].

Although countless dynamic models have been developed, solutions based on numerical methods are predominantly used. Studies presenting analytical solutions are much rarer. Among such studies are those presented in publication [20]. The article presents the system physical (mechanical) model and the derivation of the equations of motion. On this basis, the authors analytically determined linear solutions, constituting a mathematical description of vibrations. Furthermore, the publication compares the results of a numerical solution determined from nonlinear equations. It proposes various effects, such as time-varying mesh stiffness, gear profile error, equivalent error, and the influence of static load.

Research has increasingly shifted focus towards a more accurate understanding of gear dynamics by incorporating time-varying mesh stiffness. Departing from traditional quasi-static approaches, these investigations highlight the significance of nonlinear relationships between mesh stiffness and dynamic forces, particularly in spur gear systems analyzed in [8]. An interesting example is also presented in article [21], which concerns dynamic modeling of a harmonic drive in a gear transmission system, considering nonlinear changes in stiffness and damping. This contributes to expanding knowledge about torsional vibrations occurring in this type of power transmission system.

Research based on dynamic models is becoming increasingly important in the development of vibroacoustic diagnostic methods for gears, which are commonly used components in power transmission systems [22–25]. Early identification of degradation processes is essential for planning inspections and repairs, and thus for improving the reliability of all kinematic chain elements. Simulation and experimental studies presented in paper [26] have shown that the use of an identified dynamic model of a gear in a power transmission system allows reliable diagnostic relationships to be obtained for a reliable condition assessment. It is worth noting that, based on simulations and experimental studies, the authors have developed a set of neural network classifiers for diagnosing the type and severity of gear damage with a validation error of less than 5%. It should also be emphasized that condition monitoring is particularly important for preventing unplanned outages in high-value rotating machinery used in power engineering and mining [25], as well as in aerospace. In this regard, advanced and sophisticated diagnostic techniques have been developed by researchers and experts. For example, enhancing gearbox vibration signals by combining a whitening procedure and a synchronous processing method [27] or variational mode decomposition and a convolutional neural network for gearbox fault identification [28].

Expanding the scope of analysis, research has explored the influence of additional degrees of freedom in gear systems, revealing diverse behaviors in nonlinear vibration, as presented in [29]. This expanded analysis has proven instrumental in uncovering nuanced aspects of gear dynamics. For instance, to reveal failure mechanisms and investigate local damage in gear systems, the authors of article [22] proposed a 24-DOF dynamic coupling model that considers shafts, bearings and gears. This model can simulate local defects in various locations and provide data and a modeling method for diagnostics.

An article undoubtedly worthy of attention is the work of [30]. The issue of vibrations in a spur gear was analyzed. The article presents considerations on a single-degree-of-freedom (SDOF) linear system in which manufacturing errors and gear stiffness described by a parabolic relationship are considered, which is an effective approach to this issue. The authors used spectral methods and Green's function to determine the system steady-state vibrations. Based on this, the calculated eigenvalues could assess the system stability. It should be emphasized that the proposed technique can also be used to solve the problem of a complex description of the varying mesh stiffness. Furthermore, the results obtained were verified using the Floquet method, and stability maps were created. Finally, the results obtained were compared with a numerical solution, which showed a very high level of compliance for all cases considered. Sophisticated models examining time-dependent mesh stiffnesses in planetary gear trains have provided valuable insights into dynamic tooth loads, as shown in [13, 31–34]. The publications described show an analytical approach where calculations are performed manually, or computational scripts are used as a direct equivalent of manual calculations (only valid for the case under consideration). This indicates a lack of dedicated tools to support this type of computation in the general case.

Although there is no shortage of research on dynamic models of helical gears that focuses on finding analytical solutions, there is still an insufficient number of such studies, and they do not cover all issues. In this paper, the authors have addressed the issue and aim to demonstrate the effectiveness and highlight the advantages of analytical over numerical methods when analysing the dynamics of gears. The aim is to confirm the effectiveness of the analytical approach and the cost-effectiveness of its use in terms of time complexity. Particular focus is given to computation time.

The practical aspects of the proposed methodology for an approximate analytical solution of the gear meshing problem based on MSM can be highlighted as follows:

- The meshing force (inter-tooth force) has a significant impact on gear vibrations, and the mathematical model allows for a better understanding of the vibration response structure.
- This can be used in practice to better determine dynamic surpluses for more accurate gear calculations (reducing iterations in the gear pair design process).
- In addition, an interesting area of application is gear diagnostics, where knowledge of the vibration structure is a key factor for effective fault and defect detection.

The established dynamic model, as well as an analytical approach, may provide a theoretical basis for the fault diagnostics of gear transmission systems, according to recent findings [22].

2. DYNAMIC MODEL OF HELICAL GEAR

The analysis of the gear mesh dynamics requires numerical computations and simulation investigation. Table 1 lists the parameters of the helical gear used in this study.

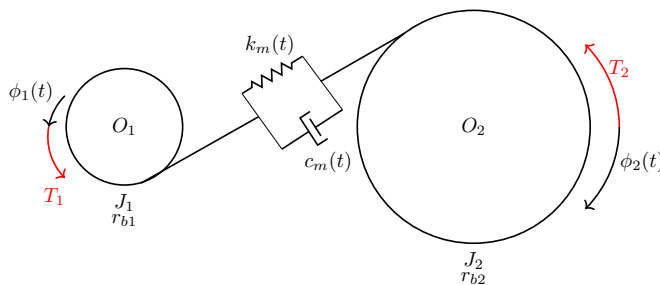
The gear dynamic model (Fig. 1) represents an isolated system oriented on the internal factors influencing its vibration behavior. This model includes only two interacting gears, each

Table 1

Basic parameters of helical gear

	Symbol	Value	Unit
Number of teeth of the pinion	z_1	26	—
Number of teeth of the gear	z_2	53	—
Module (gear system parameter)	m_n	2	mm
Center distance of the pinion	d_1	52	mm
Center distance of the gear	d_2	106	mm
Gear ratio	u	2.04	—
Pressure angle	α_{wt}	20	°
Pitch diameter of the pinion	d_{b1}	48.864	mm
Pitch diameter of the gear	d_{b2}	99.607	mm
Face width ratio	ϵ_α	1.412	—
Length of the contact line	g_α	8.338	mm
Rotational speed of the pinion	n_1	1460	rpm
Input torque	T_1	98.12	Nm

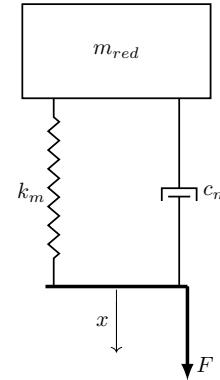
characterised by base radii r_{bi} and mass moments of inertia J_i ($i = 1$ for the pinion, $i = 2$ for the gear). The pinion is subjected to a constant input torque T_1 , while the gear is subjected to an output torque T_2 . Two parallelly connected elements with elastic-damping characteristics represent the interaction between the gears, depicting time-varying mesh stiffness $k_m(t)$ and variable damping $c_m(t)$. The proposed dynamic model of the helical gear includes two-degrees-of-freedom ($\phi_1(t)$ and $\phi_2(t)$), corresponding to the pinion and gear rotational motion.

**Fig. 1.** Dynamic model of the single-stage helical gear as a 2-DOF isolated model

The gear system can be simplified to a single equivalent body with a mass m_{red} (Fig. 2). In this case, the equivalent system undergoes a translational oscillatory motion along the x -axis, and an equivalent force F replaces (consolidates) the torques. This operation is possible because the kinematic properties of gear meshing under investigation are only within the scope of interest. The introduction of the relative generalized coordinate allows the model to be reduced to a single-degree-of-freedom (SDOF).

Kinetic energy of the system is as follows:

$$T = \frac{J_1 \dot{\phi}_1^2}{2} + \frac{J_2 \dot{\phi}_2^2}{2}. \quad (1)$$

**Fig. 2.** Dynamic model of a single-stage helical gear as a 1-DOF reduced model

Potential energy of the system is as follows:

$$V = \frac{k(-r_1\phi_1 + r_2\phi_2)^2}{2}. \quad (2)$$

Dissipative function of the system is as follows:

$$D = \frac{c(r_1\dot{\phi}_1 - r_2\dot{\phi}_2)^2}{2}. \quad (3)$$

Lagrangian of the system:

$$L = \frac{J_1 \dot{\phi}_1^2}{2} + \frac{J_2 \dot{\phi}_2^2}{2} - \frac{k(-r_1\phi_1 + r_2\phi_2)^2}{2}. \quad (4)$$

Partial derivatives:

$$\frac{\partial T}{\partial \dot{\phi}_1} = J_1 \dot{\phi}_1, \quad (5)$$

$$\frac{d}{dt} \frac{\partial T}{\partial \dot{\phi}_1} = J_1 \ddot{\phi}_1, \quad (6)$$

$$\frac{\partial T}{\partial \phi_1} = 0, \quad (7)$$

$$\frac{\partial V}{\partial \phi_1} = -kr_1(-r_1\phi_1 + r_2\phi_2). \quad (8)$$

The equation for the second coordinate is as follows:

$$\frac{\partial T}{\partial \dot{\phi}_2} = J_2 \dot{\phi}_2, \quad (9)$$

$$\frac{d}{dt} \frac{\partial T}{\partial \dot{\phi}_2} = J_2 \ddot{\phi}_2, \quad (10)$$

$$\frac{\partial T}{\partial \phi_2} = 0, \quad (11)$$

$$\frac{\partial V}{\partial \phi_2} = kr_2(-r_1\phi_1 + r_2\phi_2). \quad (12)$$

The Euler-Lagrange formula can be written in the following form:

$$\frac{\partial V}{\partial \phi_1} + \frac{d}{dt} \frac{\partial T}{\partial \dot{\phi}_1} - \frac{\partial T}{\partial \phi_1} = Q. \quad (13)$$

K. Twardoch, K. Kaczmarzyk, G. Długopolski, and B. Chilinski

$$\begin{aligned}
 \kappa_{\text{mesh}} = & 0.21 \sin\left(\frac{30\pi t}{T}\right) + 0.17 \sin\left(\frac{38\pi t}{T}\right) + 0.29 \sin\left(\frac{22\pi t}{T}\right) \\
 & + 0.64 \sin\left(\frac{10\pi t}{T}\right) + 0.46 \sin\left(\frac{14\pi t}{T}\right) + 1.1 \sin\left(\frac{6\pi t}{T}\right) \\
 & + 0.35 \sin\left(\frac{18\pi t}{T}\right) + 0.19 \sin\left(\frac{34\pi t}{T}\right) + 3.2 \sin\left(\frac{2\pi t}{T}\right) \\
 & + 0.24 \sin\left(\frac{26\pi t}{T}\right).
 \end{aligned} \quad (22)$$

The implemented dynamic system allows for a very effective analysis of the system dynamics. This type of implementation is a scalable and efficient solution. It allows for quick determination of the equations of motion or basic dynamic characteristics as follows:

```

1 gear_dsys = EquivalentGearModel()
2 eom_gear=gear_dsys.eoms
3
4 display(eom_gear.as_eq_list()[0])
5
6 %
7

```

The result is an equation displayed in a clear mathematical notation representing this object. This functionality has been achieved by using elements from the SymPy library [42] as a symbolic calculation engine (back-end).

$$-F + c_g \dot{z} + m_{\text{eq}} \ddot{z} + k_g (\kappa_{\text{mesh}} \varepsilon + 1) z = 0, \quad (19)$$

where

κ_{mesh} – formula representing stiffness variation (Fourier expansion of rectangular signal)
 c_g – mesh damping coefficient
 m_{eq} – equivalent mass
 k_g – mesh stiffness coefficient
 ε – small parameter
 z – gear vibration displacement
 \dot{z} – gear vibration velocity
 \ddot{z} – gear vibration acceleration
 F – excitation force

Another method (only implemented within the class `EquivalentGearModel` – local interface) allows for the determination of various stiffness models. Any number of models can be defined. The listing shows a model selection with the key waves.

```

1 gear_dsys = EquivalentGearModel()
2 stiff_models = gear_dsys._stiffness_models()
3
4 display(stiff_models['waves']) # reference model (HA)
5 display(stiff_models['rect']) # rectangular model (RA)
6 display(stiff_models['approx']) # Fourier approximation (FA)
7
8 %
9

```

All models considered have the following form:

$$\begin{aligned}
 \kappa_{\text{mesh}} = & -0.5 + 2.5 \text{sign}\left(\sin\left(\frac{2\pi t}{T}\right)\right) \\
 & + 1.0 \sin\left(\frac{2\pi t}{T}\right) \text{sign}\left(\sin\left(\frac{2\pi t}{T}\right)\right),
 \end{aligned} \quad (20)$$

$$\kappa_{\text{mesh}} = 2.5 \text{sign}\left(\sin\left(\frac{2\pi t}{T}\right)\right), \quad (21)$$

The mathematical dependencies (20)–(22) form the basis of the simulations presented. They were selected as example dependencies describing the variability of TVMS. Equations are presented in the form of the plot visible in Fig. 3.

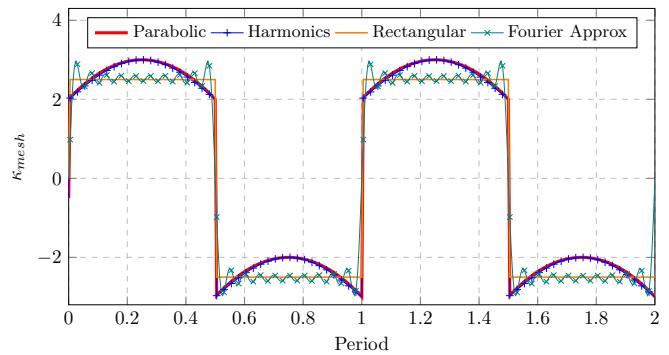


Fig. 3. Mesh stiffness models

Figure 3 compares the various mesh stiffness models used in the simulation studies.

- Parabolic reference approximation (PRA) – a mesh stiffness model where the course is a typical approximation pattern using a parabolic function.
- Harmonics approximation (HA) – a mesh stiffness model based on a periodic function as a quasi-parabolic approximation: considered an adequate matching of the mesh stiffness course pattern.
- Rectangular approximation (RA) – a mesh stiffness model based on a rectangular approximation: considered a less suitable and lower accuracy matching of the mesh stiffness course pattern compared to harmonic approximation.
- Fourier approximation (FA) – a mesh stiffness model as an approximation of the mesh stiffness course pattern also proposed in this study: sufficiently good due to frequent response for simulation studies (see study [37]).

Trigonometric functions are necessary for the proposed model application in MSM. The Fourier series expansion can be determined to obtain an expression containing only \sin and \cos functions for each periodic function. The formulas for the series expansion are as follows:

$$k_p = \frac{a_0}{2} + \sum_{n=1}^{\infty} \left(a_n \cos\left(\frac{\pi n k_p}{T}\right) + b_n \sin\left(\frac{\pi n k_p}{T}\right) \right), \quad (23)$$

where

$$a_0 = \frac{\int_{-T}^T k_p dt}{T}, \quad (24)$$

$$a_n = \frac{2 \int_{-T}^T k_p \cos\left(\frac{\pi n t}{T}\right) dt}{T}, \quad (25)$$

$$b_n = \frac{2 \int_{-T}^T k_p \sin\left(\frac{\pi n t}{T}\right) dt}{T}. \quad (26)$$

The results obtained do not contain odd components. The dependencies considered represent the variability of stiffness over time, which allows for a simplification of the analysis. The period is a variable parameter, therefore the analysis is carried out in the period domain. Numerical transformation algorithms for the frequency domain available in the DynPy library were used. It can be concluded that any periodic model can be simplified in this way to an analytical form. The proposed approach allows for assessing the convergence of different models – easy to add when creating a dynamic system.

Based on the study presented in paper [37], all computations were performed for the helical gear parameters listed in Table 1. Equation (19) was used as a base for numerical analysis of the adopted stiffness models (Fig. 3). A series of analyses was carried out. The investigation results are presented in Figs. 4 and 5 (as subplots).

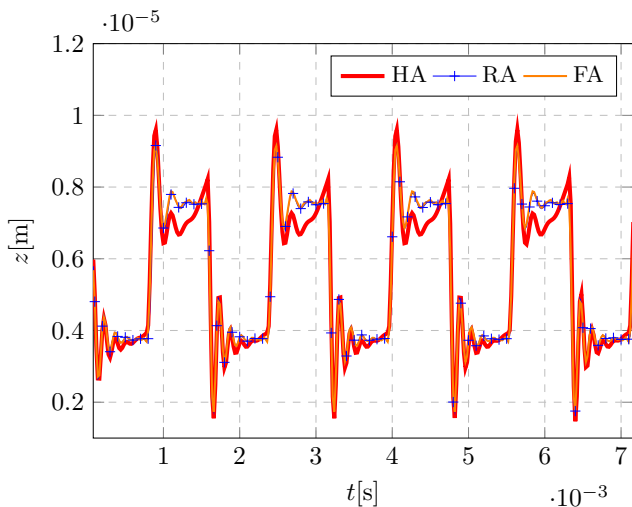


Fig. 4. Vibration displacement in gear mesh system for TVMS models: HA – harmonics approximation, RA – rectangular approximation, FA – Fourier approximation

Figures 4 and 5 compare the simulation results obtained for different approximations of mesh stiffness: harmonic (HA), rectangular (RA), and Fourier (FA) approximation. The simulations have been performed for the same period to eliminate uncertainties regarding the frequency of the signals and to enable a direct comparison of course shapes and amplitudes. It can be

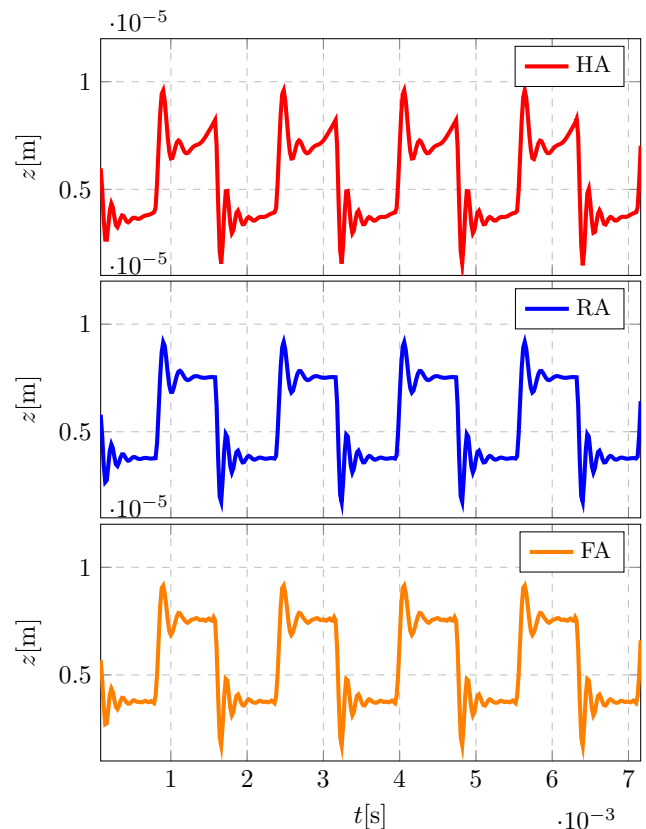


Fig. 5. Vibration displacement in gear mesh system for TVMS models: HA, RA, and FA (subplots from Fig. 4)

observed that the course amplitudes appropriate for single-tooth and double-teeth meshing are similar, but the differences in the course shapes are clear. It is worth noting that the FA approximation additionally contains signal modulation, which increases the amount of information transferred.

The parabolic model, widely recognized in the literature as a classical representation of mesh stiffness, is considered a reliable mathematical depiction of actual stiffness behavior along the path of contact. Its accuracy in scholarly discussions is well-established. The HA model serves as a close approximation to the parabolic model and demonstrates high accuracy. On the other hand, the displacement characteristics generated by the HA model are approximate those observed in the parabolic model within the time-domain. In contrast, the RA and FA models exhibit certain limitations due to additional simplifications. These models exclude the parabolic segments observed in the time-domain representation, as clearly illustrated in Fig. 5, but still sufficiently represent the fundamental gear meshing phenomena.

The RA mesh stiffness signal inherently provides lower accuracy when directly compared with the HA approximation. However, employing a Fourier series expansion in the FA model notably smooths the stiffness variations. Despite this effect, local discrepancies remain, as displacement magnitudes may be artificially exaggerated or diminished at specific time-domain intervals. Furthermore, an intrinsic challenge emerges when using the Fourier series approximation: it becomes impossible to eliminate artificial mesh stiffness overshoots entirely. These

overshoots are attributed to the Gibbs phenomenon, a fundamental feature of Fourier series expansions of periodic functions.

The equivalent force of the inter-tooth interaction can be calculated in the following way (27):

$$q_{\text{eq}} = \frac{F_c}{m_{\text{eq}}} = \frac{c_g \dot{z}}{m_{\text{eq}}} + \frac{k_g z}{m_{\text{eq}}}, \quad (27)$$

where

q_{eq} – equivalent mesh force;

F_c – mesh force.

The equivalent mesh force (27) can be rearranged to the following form:

$$q_{\text{eq}} = \omega_0^2 z + 2h\dot{z}, \quad (28)$$

where

ω_0^2 – natural frequency;

h – damping coefficient.

Figures 6 and 7 show the evolution of dynamic mesh forces and their frequency spectra for the TVMS models, respectively, including damping along the path of contact.

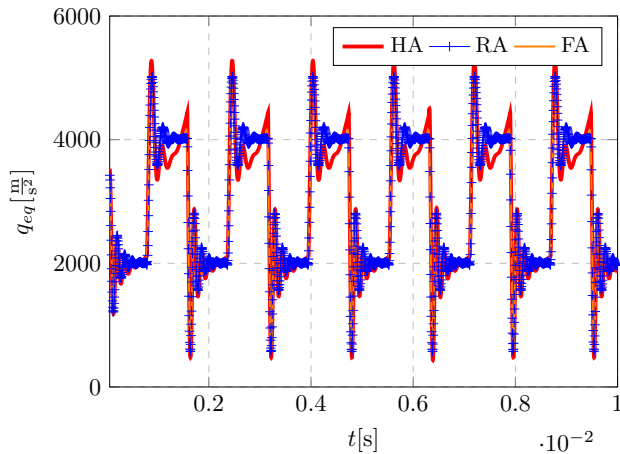


Fig. 6. Dynamic mesh forces along the path-of-contact for TVMS models: HA, RA, and FA

The dynamic effects observed for time-varying equivalent mesh force (Fig. 6) originate primarily from damping phenomena inherent within the gear mesh system. Characteristic changes in the time distribution of the mesh force manifest as periodic variations directly correlated with mesh stiffness (suitable TVMS model) – as depicted in Fig. 5.

The mesh force distribution exhibits distinct rapid increases at moments when a single pair of teeth initiates meshing engagement. The gear mesh force attains its peak values at these specific temporal points. Conversely, periods during which two pairs of teeth simultaneously remain meshing within the path of contact are associated with relatively lower force values. This lower mesh force interval extends from entering to exiting the path of contact with a double pair of teeth (during double-tooth meshing until disengagement of one pair). A rapid force's rise recurs as the mesh interaction transitions back to a single-tooth meshing.

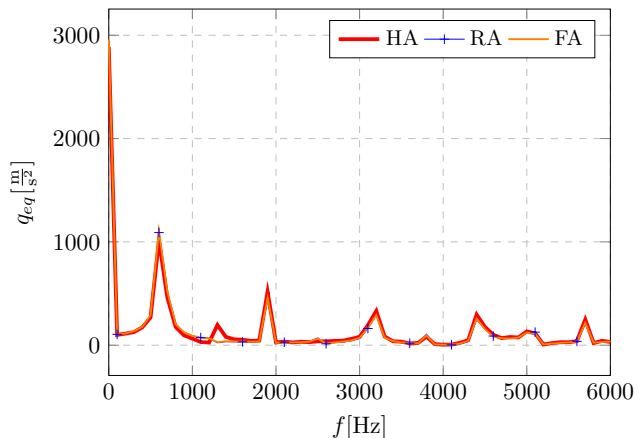


Fig. 7. Frequency spectra of dynamic mesh forces along the path of contact for TVMS models: HA, RA, and FA

4. ANALYTICAL SOLUTION

The reduced model (29) can be simplified for further analysis [37]. To improve the efficiency of calculations and to avoid multiple executions of complex ones, a computational environment created by the authors is used. This environment is based on the DynPy library and uses Jupyter Notebook, as described above in this paper. The use of the appropriate sequence of methods allows the equation (29) to be determined in a way that is convenient for further analysis. The base code is as follows:

```

1
2 dsys = EquivalentSDOFGearModel()
3
4 t, z, k, eps=dsys.ivar, dsys.z, dsys.k, dsys.eps
5 c=dsys.c
6 F=dsys.F
7 k_var=dsys.k_var
8 T=dsys.T
9 m=dsys.m
10
11 delta = Symbol('delta', positive=True)
12 omg = Symbol('omega', positive=True)
13 u_s = Symbol('u_s', positive=True)
14 mu = Symbol('mu', positive=True)
15
16 counter=13
17 data={
18     k:counter**2*omg**2,
19     c:mu*eps,
20     T:2*pi/omg,
21     m:1,
22     F:counter**2*omg**2*u_s,
23     k_var:1,
24     omg:1,
25
26
27 msm_ode=gear_dsys.approx_rect(4, numerical=True),
28     ode_with_delta().subs(data)
29     }
30
31 %

```

The code presented allows for a convenient representation of the differential equation in a form ready for perturbation

expansion. The result of the execution is as follows:

$$-F + c_g \dot{z} + m_{eq} \ddot{z} + k_g (\varepsilon (2.27 \sin(\omega t) + 0.757 \sin(3\omega t)) + 1) z + \delta k_g \varepsilon z = 0, \quad (29)$$

where

u_s – static deflection;

δ – detuning parameter;

ω – meshing frequency.

The obtained result represents a recursive system of perturbation equations determined by the multiple time scale method (MTSM). This problem is solved recursively [43]. It was assumed that the initial system of equations would be the representation of the MTSM system in Jupyter Notebook (graphical representation). The DynPy library allows us to effectively obtain the final solution. The intermediate expressions necessary to obtain the final approximate solution are also possible to analyze. The code responsible for creating the MTSM system is as follows:

```

1 msm_ode=gear_dsys.approx_rect(4,numerical=True).
2   ode_with_delta().subs(data)
3 msm_ode_subs = msm_ode.odes[0].subs({omg:1,delta:
4   delta}).subs({z:(z+u_s)}).subs({}).doit().expand()
5
6 gear_ode_msm = MultiTimeScaleSolution(msm_ode_subs,
7   ode.dvars[0],
8   ivar=ode.ivar,
9   omega=S.One, order=1, eps=eps)
10
11 %

```

The presented code creates an object of the class `MultiTimeScaleSolution`. The result of the code execution is as follows:

$$169z + \mu\varepsilon\dot{z} + 169\delta u_s \varepsilon + 169\delta\varepsilon z + 128.0u_s \varepsilon \sin(3t) + 128.0\varepsilon z \sin(3t) + 384.0u_s \varepsilon \sin(t) + 384.0\varepsilon z \sin(t) + \ddot{z} = 0, \quad (30)$$

where

u_s – static deflection;

δ – detuning parameter;

ω – meshing frequency.

By calling the corresponding methods on the instance describing the MTSM equation (30), all subsequent solving steps can be obtained. The following executions are possible:

```

1 gear_ode.predicted_solution_without_scales(3)
2 gear_ode.predicted_solution(3)
3
4 nonlin_ode_base._scales_formula
5
6 nth_ord_approx_list = nonlin_ode_base.
7   eoms_approximation_list()
8 nth_ord_approx_list[0]
9 nth_ord_approx_list[1]
10
11 %

```

The last three executions are responsible for determining the perturbation expansion for the differential equation under consideration (30). They are formed as successive elements of the equation expansion in a power series of the small parameter ε . The zeroth-order and first-order linear approximation (perturbations) have a form of equations (31) and (32):

$$169z_0(t_0, t_1) + \frac{d^2}{dt_0^2}z_0(t_0, t_1) = 0, \quad (31)$$

$$\begin{aligned} 2 \frac{d^2}{dt_1 dt_0}z_0(t_0, t_1) + 169z_1(t_0, t_1) + \mu \frac{d}{dt_0}z_0(t_0, t_1) \\ + 169\delta u_s + 169\delta z_0(t_0, t_1) \\ + 128.0u_s \sin(3t_0) + 128.0z_0(t_0, t_1) \sin(3t_0) \\ + 384.0u_s \sin(t_0) + 384.0z_0(t_0, t_1) \sin(t_0) \\ + \frac{d^2}{dt_0^2}z_1(t_0, t_1) = 0. \end{aligned} \quad (32)$$

The environment created during the execution of the work allows for the rapid construction of approximations, as shown by the equations (31) and (32). The obtained results were compared with the reference analytical calculations, confirming the effectiveness of the proposed method [18, 20, 30, 37, 44]. The differences in the results obtained are due to the different transformation techniques. Finally, the solution (displacements and speed) was determined in the following form:

$$\begin{aligned} z = C_1(t_1) \sin(13t_0) + C_2(t_1) \cos(13t_0) - \delta u_s \varepsilon \\ + 7.68\varepsilon C_2(t_1) \sin(12t_0) + 0.736\varepsilon C_2(t_1) \sin(16t_0) \\ + 7.12\varepsilon C_2(t_1) \sin(14t_0) + 0.927\varepsilon C_2(t_1) \sin(10t_0) \\ - 2.29u_s \varepsilon \sin(t_0) - 7.68\varepsilon C_1(t_1) \cos(12t_0) \\ - 0.736\varepsilon C_1(t_1) \cos(16t_0) - 0.8u_s \varepsilon \sin(3t_0) \\ - 7.12\varepsilon C_1(t_1) \cos(14t_0) - 0.927\varepsilon C_1(t_1) \cos(10t_0), \end{aligned} \quad (33)$$

$$C_1(t_1) = \left(C_1 \cos\left(\frac{13\delta t \varepsilon}{2}\right) - C_2 \sin\left(\frac{13\delta t \varepsilon}{2}\right) \right) e^{-\frac{\mu t \varepsilon}{2}}, \quad (34)$$

$$C_2(t_1) = \left(C_1 \sin\left(\frac{13\delta t \varepsilon}{2}\right) + C_2 \cos\left(\frac{13\delta t \varepsilon}{2}\right) \right) e^{-\frac{\mu t \varepsilon}{2}}, \quad (35)$$

where

C_1, C_2 – integration constants.

$$\begin{aligned} \dot{z} = 13.0C_1(t_1) \cos(13t_0) - 13.0C_2(t_1) \sin(13t_0) \\ + 11.8\varepsilon C_1(t_1) \sin(16t_0) + 11.8\varepsilon C_2(t_1) \cos(16t_0) \\ + 9.28\varepsilon C_1(t_1) \sin(10t_0) + 9.28\varepsilon C_2(t_1) \cos(10t_0) \\ + 92.2\varepsilon C_1(t_1) \sin(12t_0) + 92.2\varepsilon C_2(t_1) \cos(12t_0) \\ + 99.6\varepsilon C_1(t_1) \sin(14t_0) + 99.6\varepsilon C_2(t_1) \cos(14t_0) \\ - 2.29u_s \varepsilon \cos(t_0) - 2.4u_s \varepsilon \cos(3t_0). \end{aligned} \quad (36)$$

The obtained results are consistent with the current state of the art [37]. They differ mainly in the form of the integration constants. This is a very complex expression, and its manual analysis is difficult. The code used facilitates the solution of the computational problem. The obtained results are consistent with

similar publications that treat problems of analytical investigation of parametric vibration considering the time-variable mesh stiffness. The proposed methodology, based on object-oriented programming, makes the problem computationally efficient and improves the quick obtaining results. The time complexity of the calculations decreases, reducing the computational cost.

5. MODEL SENSITIVITY ANALYSIS TO CHANGES IN MESH PARAMETERS

5.1. Calculation environment for analysis

A sensitivity analysis was carried out to analyze the gear dynamics in more detail and to obtain reference data. A numerical system of motion equations was developed using the dynamic models implemented in the work. The LSODA algorithm provided by the SciPy library [45] was chosen for the simulation. The used environment is based on the Python programming language, which increases computing performance. This allows each solution to be efficiently implemented within the basic programming structures. For this purpose, a procedure to automate the execution of the sensitivity analysis for the selected parameter was written. This procedure code is as follows:

```

2 k_values=[3*10**8,6*10**8,9*10**8,1*10**9]
3 c_values=[3*10**3,6*10**3,3*10**4,6*10**4]
4 m_values=[.3,.6,1,2]
5
6 def perform_sensitivity_analysis(param,param_span,
7     name,t_span,reference_data):
8
9     data_dict_param = {**reference_data,param:param}
10
11    na_df3 = dyn_sys.subs(data_dict_param)(name).
12    numerical_analysis(parameter=param,coordinates
13    =2,
14
15                t_span=t_span,
16
17                param_span=param_span
18
19            )
20
21    results = na_df3.perform_simulations(backend='
22    numpy')
23
24
25    return results
26
27
28    %

```

The prepared environment allows for numerical simulations for any shape of the TVMS approximation function. It was decided to carry out simulations with a parabolic TVMS signal to compare the effectiveness of the proposed solution with the results of the research presented in the paper [37], where simulations based on the Fourier approximation of the rectangular TVMS signal were carried out.

Using the capabilities of the created environment, a preliminary comparison of the displacements z , velocities \dot{z} , and accelerations \ddot{z} during the simulation (gear operation) was made. The results obtained in the time-domain (Figs. 8–11) and the frequency domain (Figs. 12–14) allowed us to select the most interesting simulation results. The reference values of the system's parameters are contained in Table 2.

Table 2
Reference values of the parameters for simulations

	Symbol	Value	Unit
Stiffness	k_g	8.0e+8	N/m
Force	F	4.0e+3	N
Damping	c_g	9.0e+3	Ns/m
Period	T	0.0016	s
Mass	m_{eq}	0.57	kg
Small parameter	ε	0.13	—

5.2. Effect of mesh stiffness, k_s

The numerical investigation of these approximated analytical solutions began with a stiffness analysis. Figure 8 shows the time-varying displacement for four mesh stiffness (k_g) values.

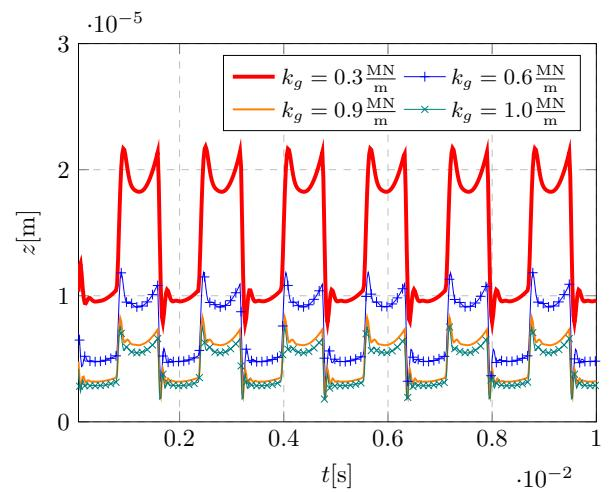


Fig. 8. Time-history of vibration displacement in gear mesh system for selected mesh stiffness coefficients

Vibrations displacement based on the time-domain signals in Figs. 8 and 9 (as subplots) show that the lower the mesh stiff-

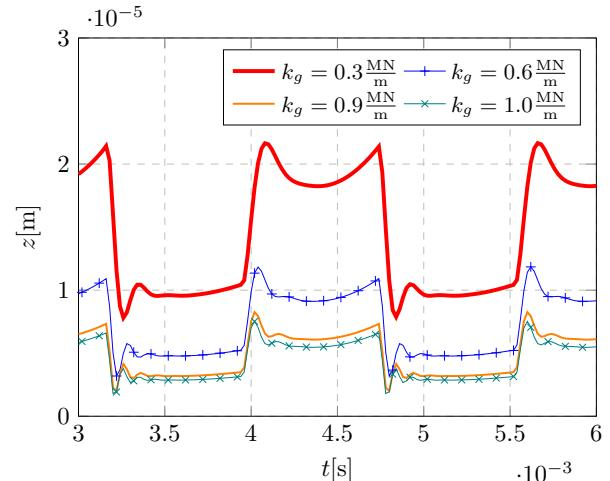


Fig. 9. Time-history of vibration displacement in gear mesh system for selected mesh stiffness coefficients: signal qualitative zoom from Fig. 8 (narrow the time-domain)

ness, the higher the vibration amplitude. The amplitude variability corresponds directly to the changes in the mesh stiffness, whereby the vibration period remains the same.

On the other hand the results in Fig. 10 show:

- The signals of velocity in the time-domain reveal a more dynamic transient behavior than the displacement, with amplitudes increasing at sudden changes in mesh stiffness.
- At higher mesh stiffness, the speed oscillations decay faster, which means better vibration energy dissipation.
- Analysis of the obtained results (presented in the figures) reveals that decrease of the parameter k_g from 0.90 to 0.30 N/m results in change of the acceleration level from 3.9E+3 to 5.0E+3 m/s². It means that parameter increases 1.3E+2% (1.3 times).

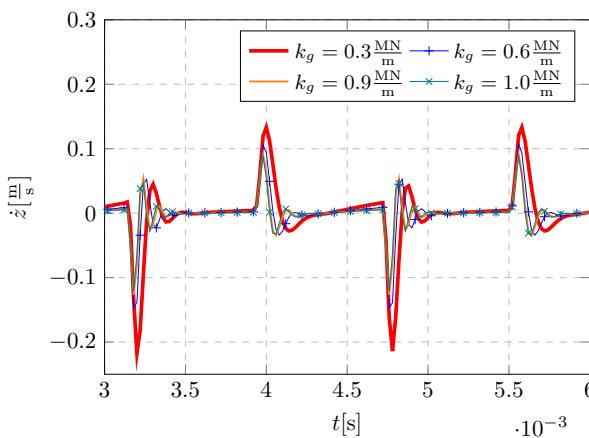


Fig. 10. Time-history of vibration velocity in gear mesh system for selected mesh stiffness coefficients: signal qualitative zoom (narrow the time-domain)

In turn, an analysis of the results in Fig. 11 reveals:

- The acceleration of the vibrations in the time-domain maintains constant amplitude values regardless of the mesh stiffness. Still, in transient states, the amplitude increases rapidly, which is related to the constant value of the force loading the gears.

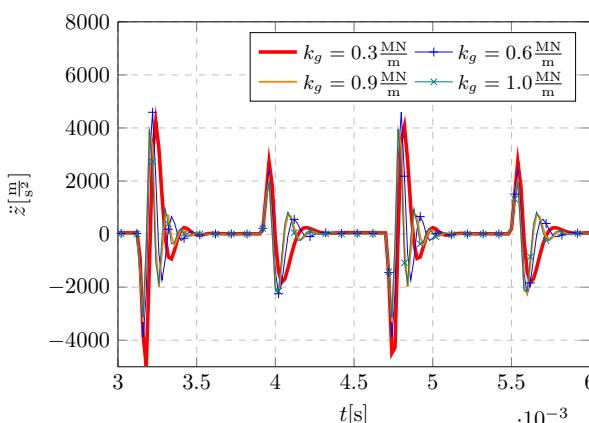


Fig. 11. Time-history of vibration acceleration in gear mesh system for selected mesh stiffness coefficients: signal qualitative zoom (narrow the time-domain)

- A particularly clear increase in the acceleration amplitude occurs when switching from single-tooth to double-tooth meshing and vice versa.

The results' analysis allows us to conclude about the higher precision of the analyzed model. The obtained results indicate dynamic behavior consistent with the known results from the literature, which allows us to claim the adequacy of the simplified model described by the selected parameters.

Spectra analysis in Fig. 12 indicates:

- The displacement frequency spectrum shows peaks at the gear mesh frequency and its multiples, and an increase in mesh stiffness reduces these values.
- Higher mesh stiffness results in better mechanical stability of the system, limiting the displacement amplitudes.

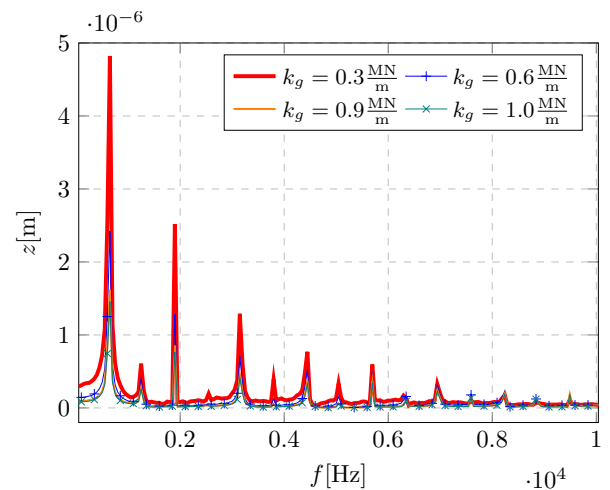


Fig. 12. Frequency spectra of vibration displacement in gear mesh system for selected mesh stiffness coefficients

However, spectral analysis in Fig. 13 allows us to conclude that:

- The frequency spectrum of the velocity shows peaks for higher harmonics, and an increase in mesh stiffness causes

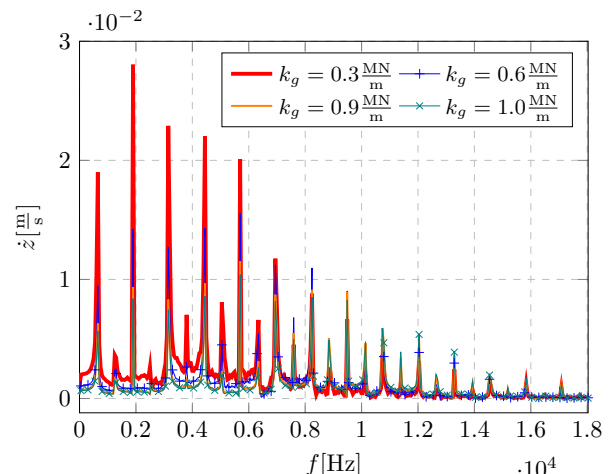


Fig. 13. Frequency spectra of vibration velocity in gear mesh system for selected mesh stiffness coefficients

the energy to be dissipated more quickly over a wider frequency range.

- Higher mesh stiffness improves the dynamic stability of the system, reducing peak velocities and ensuring smoother vibration transitions.

Figure 14 shows the system vibration acceleration in the frequency domain. Simulations performed for the parameter k_g allow to observe that if:

- $k_g = 0.30 \text{ N/m}$ then the highest value (peak) is 667.345 m/s^2 for $f = 5694.31 \text{ Hz}$.
- $k_g = 0.60 \text{ N/m}$ then the highest value (peak) is 518.154 m/s^2 for $f = 5694.31 \text{ Hz}$.
- $k_g = 0.90 \text{ N/m}$ then the highest value (peak) is 423.828 m/s^2 for $f = 9490.51 \text{ Hz}$.
- $k_g = 1.0 \text{ N/m}$ then the highest value (peak) is 392.579 m/s^2 for $f = 9490.51 \text{ Hz}$.

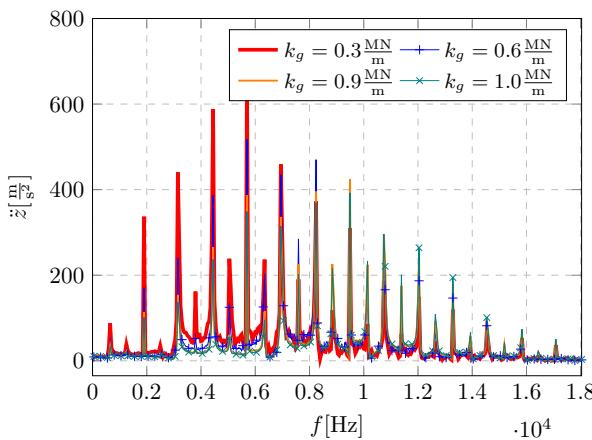


Fig. 14. Frequency spectra of vibration acceleration in gear mesh system for selected mesh stiffness coefficients

Spectra analysis in Fig. 14 reveals:

- The acceleration frequency spectrum shows dominant peaks in the meshing frequency, and the higher stiffness causes an increased energy concentration at higher frequencies.
- Higher mesh stiffness reduces peak amplitudes and spreads the energy distribution, which reduces the risk of material fatigue and improves system stability.

General observations show that mesh stiffness has a significant impact on the vibration behavior of the transmission in the drive train. An increase in the mesh stiffness reduces the amplitudes of displacement, velocity, and acceleration, improving vibration stability and limiting the effects of resonance. Transitions between single-tooth and double-tooth meshing generate noticeable peaks in vibration signals, and this effect is more pronounced at lower stiffness.

5.3. Effect of equivalent mass, m_{eq}

The next study stage was to identify the impact of the equivalent mass (m_{eq}) of gears on meshing dynamics. The results in Fig. 15 allow us to conclude that:

- An increase in the system mass increases the amplitude of the displacement and changes the frequency of the oscillations, with smaller masses showing greater susceptibility to vibration.
- Higher mass causes a reduction in peak acceleration values and a shift in vibration energy to lower frequencies.
- Investigation of the resultant data (shown in the figures) allows to note that decrease in the quantity m_{eq} from 2.0 to 0.30 kg causes change in the acceleration value from $1.5E+3$ to $4.0E+3 \text{ m/s}^2$. Interpretation of this change states that increases $2.8E+2\%$ (2.8 times).

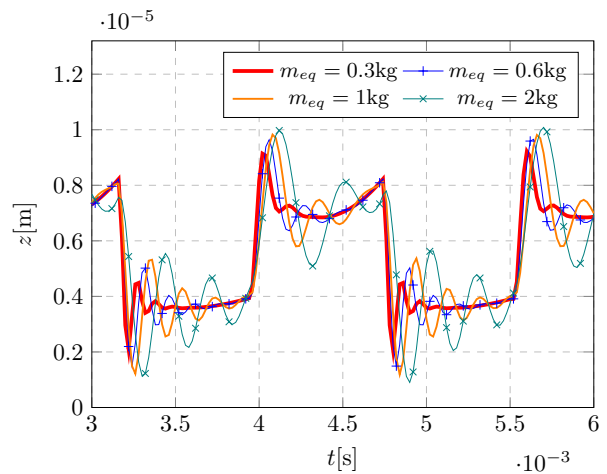


Fig. 15. Time-history of vibration displacement in gear mesh system for selected equivalent mass: signal qualitative zoom (narrow the time-domain)

An analysis of the time signals (Fig. 15) reveals if the equivalent mass (m_{eq}) increases from 0.3 to 2.0, the amplitude also increases.

Figure 16 shows the system acceleration response in the frequency domain. Simulations performed for the parameter m_{eq} allow to observe that if:

- $m_{eq} = 0.3 \text{ kg}$ then the highest value (peak) is 443.09 m/s^2 for $f = 9490.51 \text{ Hz}$.
- $m_{eq} = 0.6 \text{ kg}$ then the highest value (peak) is 460.366 m/s^2 for $f = 5694.31 \text{ Hz}$.
- $m_{eq} = 1 \text{ kg}$ then the highest value (peak) is 490.193 m/s^2 for $f = 5694.31 \text{ Hz}$.
- $m_{eq} = 2 \text{ kg}$ then the highest value (peak) is 330.6 m/s^2 for $f = 3796.2 \text{ Hz}$.

Spectral analysis in Fig. 16 shows that for smaller masses ($m_{eq} < 0.6 \text{ kg}$) the spectrum is more concentrated near the gear mesh frequency. Higher masses ($m_{eq} = 1 \text{ kg}$, and more) result in a wider range of observable peaks.

Analysis of the helical gear system for different weights allows specific trends to be observed. The influence of mass on vibration dynamics is important for gear system design. Increasing the mass improves vibration stability by reducing displacements and accelerations, acting as a natural damper. Analysis for specific simulation parameters has shown that the model is inadequate for masses above 3 kg [37].

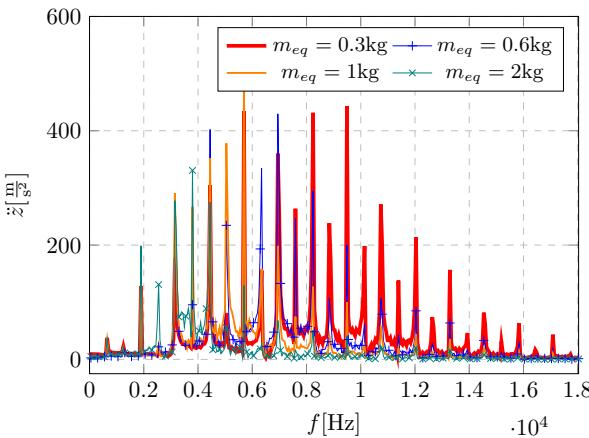


Fig. 16. Frequency spectra of vibration acceleration in gear mesh system for selected equivalent mass

5.4. Effect of mesh damping, c_g

The graphs in Fig. 17 show the system acceleration response over time for different damping coefficients. The analysis of results shows:

- An increase in the damping ratio reduces the displacement amplitudes, which accelerates the stabilization of the system and reduces oscillations.
- Higher damping values effectively dampen vibrations and dissipate energy faster, stabilizing the system.
- Investigation of the resultant data (shown in the figures) allows us to note that decrease in the quantity c_g from 60 to 3.0 N s/m causes change in the acceleration value from $1.2E+3$ to $6.6E+3$ m/s². Interpretation of this change states that it increases $5.4E+2\%$ (5.4 times).

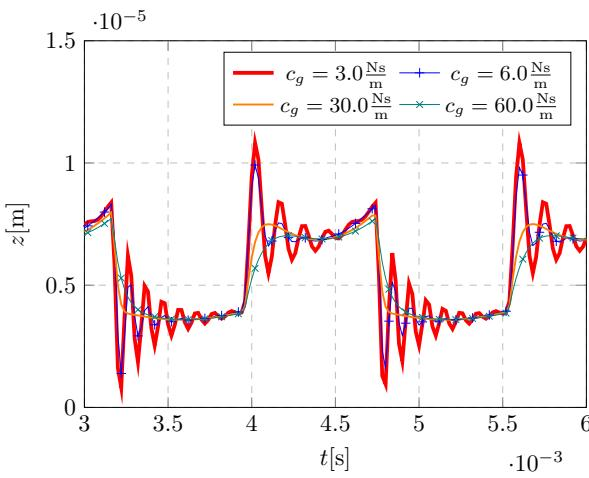


Fig. 17. Time-history of vibration displacement in gear mesh system for selected mesh damping coefficients: signal qualitative zoom (narrow the time-domain)

In a double-tooth meshing, the displacement values are lower, and the number of oscillations increases, whereas in a single-tooth meshing, the damping is less effective. High damping values limit peak amplitudes and dissipate energy over a wider frequency range, reducing the resonance risk.

In turn, Fig. 18 shows the acceleration of the system vibrations in the frequency domain for different mesh damping coefficients. Simulations performed for the parameter c_g allow to observe that if:

- $c_g = 3.0$ Ns/m then the highest value (peak) is 979.415 m/s² for $f = 9490.51$ Hz.
- $c_g = 6.0$ Ns/m then the highest value (peak) is 622.249 m/s² for $f = 9490.51$ Hz.
- $c_g = 30$ Ns/m then the highest value (peak) is 192.689 m/s² for $f = 5694.31$ Hz.
- $c_g = 60$ Ns/m then the highest value (peak) is 103.006 m/s² for $f = 5694.31$ Hz.

The shape of the FFT plot remains almost unchanged similarly to stiffness. A behavior of maximal amplitude is observed, where the acceleration decreases for increasing damping. The frequency at which the highest peak appears remains constant except for the extremely high damping value $c_g > 30.0$ N s/m.

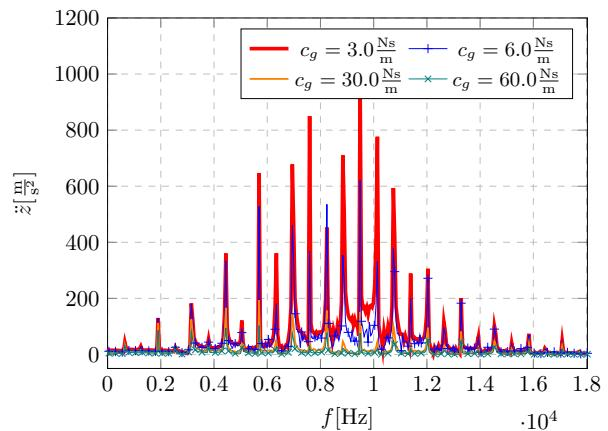


Fig. 18. Frequency spectra of vibration acceleration in gear mesh system for selected mesh damping coefficient

Spectral analysis in Fig. 18 allows us to conclude that:

- The highest acceleration peaks occur at low damping coefficients, while an increase in damping reduces the peak values.
- Higher damping disperses energy over a wider frequency range, limiting the risk of resonance and confirming the damping effect (damping efficiency).

Generally, the system stability increases with the increase of the damping coefficient, minimizing the displacement and acceleration reactions to dynamic loads. Higher damping coefficients cause a rapid decrease in acceleration amplitudes. Effective damping accelerates the reduction of vibration energy, improving the system work efficiency (system performance) and reducing mechanical fatigue. Optimizing the damping ratio is key to improving machinery reliability and lifespan.

6. ASSESSMENT OF THE OBTAINED SOLUTION

Assesment of the obtained approximated solution was based on the comparison between numerical approach and analytical results. It allows us to show the difference between these methods

and possible applications of obtained analytical solution. In order to compare results, the governing equation was transformed to the dimensionless form. It has a following form:

$$\begin{aligned}
 & 169z(\tau) + \mu\varepsilon \frac{d}{d\tau}z(\tau) + 169\delta u_s \varepsilon + 169\delta\varepsilon z(\tau) \\
 & + 128.0u_s \varepsilon \sin(3\tau) + 128.0\varepsilon z(\tau) \sin(3\tau) \\
 & + 76.7u_s \varepsilon \sin(5\tau) + 76.7\varepsilon z(\tau) \sin(5\tau) \\
 & + 384.0u_s \varepsilon \sin(\tau) + 384.0\varepsilon z(\tau) \sin(\tau) \\
 & + 54.7u_s \varepsilon \sin(7\tau) + 54.7\varepsilon z(\tau) \sin(7\tau) \\
 & + \frac{d^2}{d\tau^2}z(\tau) = 0.
 \end{aligned} \tag{37}$$

Obtained equation was solved in the way presented in the previous section and calculated for selected timestamps. A time-domain analysis was performed first, and the results are shown in Figs. 19 and 20.

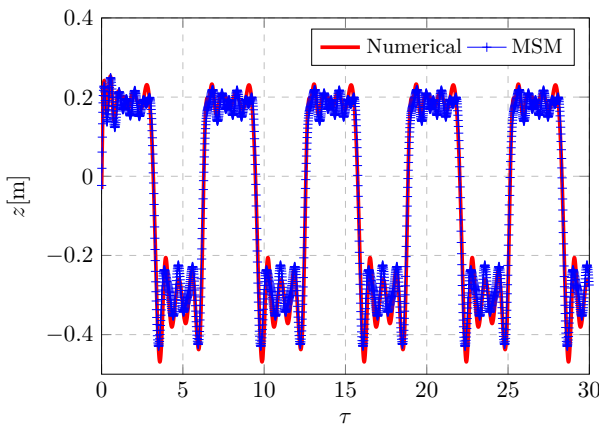


Fig. 19. Comparison of numerical and analytical solution for exemplary data

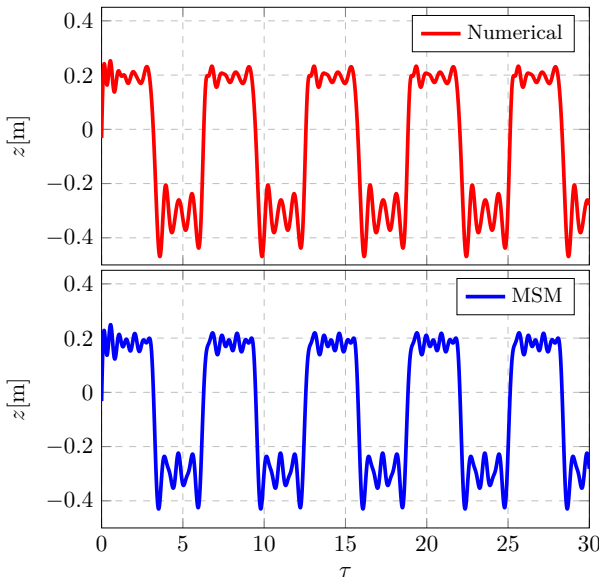


Fig. 20. Comparison of numerical and analytical solution for exemplary data (subplots)

The comparison between the numerical and analytical solutions demonstrates acceptable differences in the system displacements. These discrepancies can be attributed to the assumed order of approximated solution. The acceptable error margin below 5% (from maximal displacements comparison) is visible, however qualitative convergence is better. To confirm this statement, frequency domain analysis was done. The frequency spectrum is presented in Figs. 21 and 22.

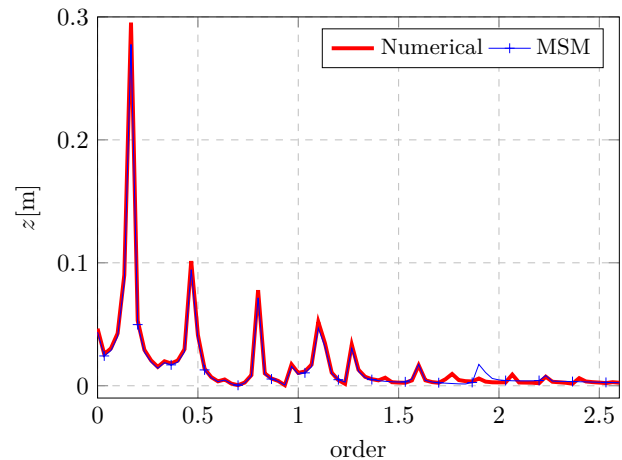


Fig. 21. Comparison of spectral analysis of numerical and analytical solution for exemplary data

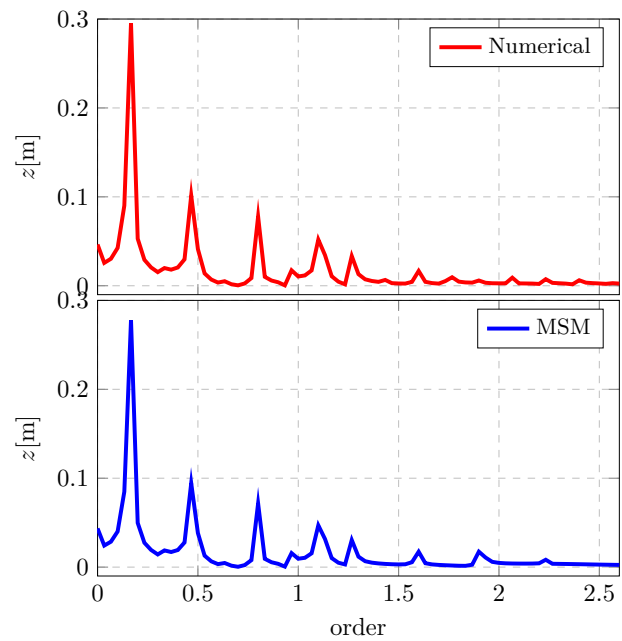


Fig. 22. Comparison of spectral analysis of numerical and analytical solution for exemplary data (subplots)

The results obtained confirm the convergence of the analytical approach. It is visible that quantitative errors are related to missing harmonical components that are caused by the assumed accuracy of prediction (attribute of perturbational approach).

For small values of the parameter ϵ , the results from both methods are nearly identical, with only minor discrepancies. Results obtained revealed a computation error. The following formula was used:

$$\Delta = \frac{A_{f1}^{\text{ana}} - A_{f1}^{\text{num}}}{A_{f1}^{\text{num}}}. \quad (38)$$

Calculated errors are approximately 6% for this assessment method, which is more reliable than maximal displacements comparison.

However, as ε increases, the differences between the two methods become more noticeable. These discrepancies manifest as a phase shift between the solutions, with the magnitude of the phase shift and the overall solution difference increasing as ε grows. This behavior highlights the limitations of the multi-scale method for larger perturbations, where higher-order effects cannot be neglected.

Overall, the analysis confirms the accuracy of the multi-scale method for small perturbations while emphasizing the need for caution when extending its use to larger values of ε .

7. CONCLUSIONS

The application of the multiple time scales method (MTSM) to model time-varying mesh stiffness (TVMS) fills pivotal gaps in the parametric vibration analysis. The main objective was to develop and verify analytical solutions and understand the frequency structure of the meshing phenomenon.

Drawing upon simulations of the helical gear system with TVMS and a comparison of analytical and numerical results, the following conclusions emerge:

1. The proposed two-degree-of-freedom model can be effectively reduced to a one-degree-of-freedom TVMS model and effectively simulates the system's behavior.
2. The proposed approach to applying spectral decomposition results ensures high convergence in the analysis of stiffness characteristics and dynamic response.
3. Minor phase shifts (due to Fourier approximation) limit precision for specific applications, such as control purposes.
4. Despite the complexity of the resulting expressions, these solutions provide valuable insight into system periodicity and amplitude modulation, supporting the overall assessment of meshing dynamics.
5. It should be noted that the analytical solution guarantees the reliability and repeatability of the results due to its explicit mathematical form. This has a direct impact on reducing the computation time.
6. The analytical solution converges with the numerical solution for the second approximation and the value of the small parameter $\varepsilon < 0.1$. Using the first approximation or the value of the small parameter $\varepsilon > 0.1$ results in a marked increase in divergence.
7. The computational framework developed for this study significantly supports the search for an analytical solution using multiple time scales by specialized methods implemented. It fills a gap in currently existing solutions.

Overall, MTSM offers a robust analytical foundation for predicting and managing parametric vibrations in gear systems. Enhancing mesh stiffness and optimizing damping improves stability, reduces oscillations, and supports gear durability. These analytical insights can be instrumental in refining helical gear design, enabling early fault detection, vibration minimization, and more sustainable, operator-friendly machinery performance.

ACKNOWLEDGEMENTS

The article was co-financed from the state budget of Poland and awarded by the Minister of Science within the framework of the Excellent Science II Programme.

APPENDIX

The code describing dynamic systems is as follows

```

class EquivalentGearModel(ComposedSystem):
    """Ready to use sample Single Degree of Freedom
    System with mass on spring
    Arguments:
    =====
        m = Mass
            -Mass of system on spring

        k = Spring coefficient
            -Spring carrying the system

        ivar = symbol object
            -Independant time variable

        qs = dynamicsymbol object
            -Generalized coordinates

    Example
    =====
    A mass oscillating up and down while being held
    up by a spring with a spring constant k

    >>> t = symbols('t')
    >>> m, k = symbols('m, k')
    >>> qs = dynamicsymbols('z') # Generalized
    Coordinates
    >>> mass = SDofHarmonicOscillator(m,k, qs=[z], )
    # Initialization of LagrangesDynamicSystem
    instance

    -We define the symbols and dynamicsymbols
    -Kinetic energy T and potential energy v are
    evaluated to calculate the lagrangian L
    -Reference frame was created with point P
    defining the position and the velocity
    determined on the z axis
    -external forces assigned
    -Next we determine the instance of the system
    using class LagrangeDynamicSystem
    -We call out the instance of the class
    -If necessary assign values for the default
    arguments

    """

```

```

m = Symbol("m_(\rm eq)", positive=True)
k = Symbol("k_g", positive=True)
F = Symbol("F", positive=True)
c = Symbol("c_g", positive=True)
T = Symbol("T", positive=True)
omega = Symbol("omega", positive=True)
ivar = Symbol("t")
k_var = Symbol("kappa_mesh", positive=True)
eps = Symbol("varepsilon", positive=True)
c_var = Symbol("c_var", positive=True)
f = Symbol("f", positive=True)

z = dynamicsymbols("z")

def __init__(self,
             m=None,
             k=None,
             F=None,
             z=None,
             c=None,
             T=None,
             ivar=None,
             k_var=None,
             eps=None,
             c_var=None,
             f=None,
             **kwargs,
             ):
    if k_var is not None:
        self.k_var = k_var
    if eps is not None:
        self.eps = eps
    if m is not None:
        self.m = m
    if k is not None:
        self.k = k
    if F is not None:
        self.F = F
    if z is not None:
        self.z = z
    if c is not None:
        self.c = c
    if T is not None:
        self.T = T
    if c_var is not None:
        self.c_var = c_var
    if ivar is not None:
        self.ivar = ivar
    if f is not None:
        self.f = f

    self.qs = [self.z]
    self._init_from_components(**kwargs)

@cached_property
def components(self):
    components = {}
    self.c_var = self.c * (1 + 0 * self.eps * self.k_var)
    stiffness = self.k * (1 + self.eps * self.k_var)

    self.gear_inertia = MaterialPoint(self.m, self.z, qs=self.qs)
    self.gear_stiffness = Spring(stiffness, self.z, qs=self.qs)
    self.force = Force(self.F, self.z, qs=self.qs)

    self.gear_damping = Damper(self.c_var, self.z, qs=self.qs)

    components["gear_inertia"] = self.gear_inertia
    components["gear_stiffness"] = self.gear_stiffness
    components["force"] = self.force
    components["gear_damping"] = self.gear_damping

    return components

def symbols_description(self):
    self.sym_desc_dict = {
        self.m: r"mass of the system on spring",
        self.F: r"excitation force",
        self.c: r"damping constant",
        self.k: r"stiffness",
        self.T: r"torque [not sure]",
    }

    return self.sym_desc_dict

def _report_components(self):
    comp_list = [*REPORT_COMPONENTS_LIST]
    return comp_list

def units(self):
    f = Symbol("f")
    units_dict = {
        self.k: ureg.newton / ureg.meter,
        self.m: ureg.kilogram,
        self.F: ureg.newton,
        self.ivar: ureg.second,
        self.T: ureg.newton * ureg.meter,
        self.z.diff(self.ivar, 2): ureg.meter / ureg.second**2,
        self.c: ureg.newton * ureg.second / ureg.meter,
        self.f: ureg.hertz,
    }
    return units_dict

def get_numerical_data(self):
    k, m, c, F, eps = symbols("k m c F epsilon", positive=True)

    default_data_dict = {
        self.k: [1e6],
        self.m: [1],
        self.c: [2e-4 * 1e6],
        self.F: [100],
        self.eps: [0.1],
    }
    return default_data_dict

def trig_stiff(self, angle=2 * pi):
    trig = sin(self.omega * self.ivar)
    new_eq = self.subs(self.k_var, trig)

    return new_eq

def wave_stiff(self):
    wave1 = (100 * (sin(self.ivar / self.T)) + 1000) * Heaviside(
        sin(self.ivar / self.T)
    )

```

```

169      wave2 = (100 * (-sin(self.ivar / self.T))) * 233
Heaviside(-sin(self.ivar / self.T)) 234
170      waves = wave1 + wave2 235
171      new_eq = self.subs(self.k_var, waves) 236
172
173      return new_eq 237
174
175  def rect_stiff(self, no=6, numerical=False): 240
176      t = self.ivar 241
177      omg = self.omega 242
178
179      trig = sum( 243
180          [Heaviside(omg * t - 1) + 0 * Heaviside( 244
omg * t - 2) for ind in range(no)] 244
181      )
182      new_eq = self.subs(self.k_var, trig) 245
183
184      return new_eq 246
185
186  def approx_rect(self, no=6, numerical=False): 247
187
188      if numerical is True: 248
189          amps_list = [ 249
190              2.27348466531425, 250
191              0, 251
192              0.757408805199249, 252
193              0, 253
194              0.453942816897038, 254
195              0, 255
196              0.323708002807428, 256
197              0, 257
198              0.25121830779797, 258
199              0, 259
200              0.204977919963796, 260
201              0, 261
202              0.172873394602606, 262
203              0, 263
204              0.149252079729775, 264
205              0, 265
206              0.131121653619234, 266
207              0, 267
208              0.116749954968057, 268
209              0, 269
210          ]
211      else: 270
212          amps_list = symbols(f"a_0:{no}") 271
213
214      rectangular_approx = sum( 272
215          [ 273
216              N(amp, 3) * sin((ind) + 1) * self. 274
omega * self.ivar) 275
217              for ind, amp in enumerate(amps_list 276
[0:no]) 277
218          ] 278
219      )
220      new_eq = self.subs({self.k_var: ( 280
rectangular_approx)}) 281
221
222      return new_eq 282
223
224  def ode_with_delta(self): 284
225      delta = Symbol("delta", positive=True) 285
226      eps = Symbol("varepsilon", positive=True) 286
227
228      with_delta = self._eoms[0] + self.k * eps * 287
delta * self.z 288
229      delta_sys = type(self._ode_system)( 289
230          with_delta, Matrix([self.z]), ivar=self. 290
ivar, ode_order=2 291
      )
231
232
233      return delta_sys
234
235  def _stiffness_models(self):
236
237      # wave
238      t = self.ivar
239      T = self.T
240
241      wave1 = (1 * (sin(2 * pi * t / T)) + 2.0) *
242          (1 / 2 + 1 / 2 * sign(sin(2 * pi * t / T))
243      )
244      wave2 = (1 * (-sin(2 * pi * t / T)) - 3.0) *
245          (1 / 2 + 1 / 2 * sign(-sin(2 * pi * t / T))
246      )
247      waves = wave1 + wave2
248
249      # rectangular
250      rectangular = 5 * ((1 / 2 + 1 / 2 * sign(sin(2 * pi * t / T))) - S.Half)
251
252      # rectangular_approx
253      amps_list = [
254          2.27348466531425,
255          0.757408805199249,
256          0.453942816897038,
257          0.323708002807428,
258          0.251218307797979,
259          0.204977919963796,
260          0.172873394602606,
261          0.149252079729775,
262          0.131121653619234,
263          0.116749954968057,
264      ]
265      rectangular_approx = sum(
266          [
267              amp * 2 / sqrt(2) * sin((2 * (no) +
268              1) * 2 * pi * t / T)
269              for no, amp in enumerate(amps_list
270              [0:])]
271          )
272
273      return {"wave": waves, "rect": rectangular,
274      "approx": rectangular_approx}
275
276  def _stiffness_waveforms(self):
277
278      from sympy import lambdify
279
280      t = self.ivar
281      T = self.T
282
283      return {
284          label: lambdify((t, T), waveform)
285              for label, waveform in self.
286      _stiffness_models().items()
287      }
288
289  %

```

REFERENCES

- [1] H. Ma, J. Zeng, R. Feng, X. Pang, and B. Wen, “An improved analytical method for mesh stiffness calculation of spur gears with tip relief,” *Mech. Mach. Theory*, vol. 98, pp. 64–80, 2016, doi: 10.1016/j.mechmachtheory.2015.11.017.

[2] P.M. Marques, J.D. Marafona, R.C. Martins, and J.H. Seabra, "A continuous analytical solution for the load sharing and friction torque of involute spur and helical gears considering a non-uniform line stiffness and line load," *Mech. Mach. Theory*, vol. 161, p. 104320, 2021, doi: [10.1016/j.mechmachtheory.2021.104320](https://doi.org/10.1016/j.mechmachtheory.2021.104320).

[3] J.I. Pedrero, M. Pleguezuelos, and M.B. Sánchez, "Analytical model for meshing stiffness, load sharing, and transmission error for helical gears with profile modification," *Mech. Mach. Theory*, vol. 185, p. 105340, 2023, doi: [10.1016/j.mechmachtheory.2023.105340](https://doi.org/10.1016/j.mechmachtheory.2023.105340).

[4] Y. Li, S. Yuan, W. Wu, X. Song, K. Liu, and C. Lian, "Dynamic analysis of the helical gear transmission system in electric vehicles with a large helix angle," *Machines*, vol. 11, no. 7, p. 696, 2023, doi: [10.3390/machines11070696](https://doi.org/10.3390/machines11070696).

[5] C.-J. Bahk and R.G. Parker, "Analytical solution for the nonlinear dynamics of planetary gears," *J. Comput. Nonlinear Dyn.*, vol. 6, no. 2, p. 021007, 2010, doi: [10.1115/1.4002392](https://doi.org/10.1115/1.4002392).

[6] J. Margielewicz, D. Gąska, and G. Wojnar, "Numerical modelling of toothed gear dynamics," *Sci. J. Silesian Univ. Technol. – Series Transport*, vol. 97, pp. 105–115, 2017, doi: [10.20858/sjst.2017.97.10](https://doi.org/10.20858/sjst.2017.97.10).

[7] Y.-C. Chen, "Time-varying dynamic analysis for a helical gear pair system with three-dimensional motion due to bearing deformation," *Adv. Mech. Eng.*, vol. 12, no. 5, p. 1687814020918128, 2014, doi: [10.1177/1687814020918128](https://doi.org/10.1177/1687814020918128).

[8] Z. Cao, Z. Chen, and H. Jiang, "Nonlinear dynamics of a spur gear pair with force-dependent mesh stiffness," *Nonlinear Dyn.*, vol. 99, no. 2, pp. 1227–1241, 2020, doi: [10.1007/s11071-019-05348-0](https://doi.org/10.1007/s11071-019-05348-0).

[9] S.M. Berri, "Gear vibration analysis: An analytical and experimental study," in *International Design Engineering Technical Conferences and Computers and Information in Engineering Conference*, vol. 6C: 18th Biennial Conference on Mechanical Vibration and Noise, 2001, pp. 3173–3180, doi: [10.1115/DETC2001/VIB-21756](https://doi.org/10.1115/DETC2001/VIB-21756).

[10] A. Fernandez del Rincon, F. Viadero, M. Iglesias, P. García, A. de Juan, and R. Sancibrian, "A model for the study of meshing stiffness in spur gear transmissions," *Mech. Mach. Theory*, vol. 61, pp. 30–58, 2013, doi: [10.1016/j.mechmachtheory.2012.10.008](https://doi.org/10.1016/j.mechmachtheory.2012.10.008).

[11] Z. Wan, H. Cao, Y. Zi, W. He, and Y. Chen, "Mesh stiffness calculation using an accumulated integral potential energy method and dynamic analysis of helical gears," *Mech. Mach. Theory*, vol. 92, pp. 447–463, 2015, doi: [10.1016/j.mechmachtheory.2015.06.011](https://doi.org/10.1016/j.mechmachtheory.2015.06.011).

[12] H. Nevzat Özgüven and D. Houser, "Mathematical models used in gear dynamics – a review," *J. Sound Vib.*, vol. 121, no. 3, pp. 383–411, 1988, doi: [10.1016/S0022-460X\(88\)80365-1](https://doi.org/10.1016/S0022-460X(88)80365-1).

[13] N. Gao, C. Meesap, S. Wang, and D. Zhang, "Parametric vibrations and instabilities of an elliptical gear pair," *J. Vib. Control*, vol. 26, no. 19-20, pp. 1721–1734, 2020, doi: [10.1177/1077546320902543](https://doi.org/10.1177/1077546320902543).

[14] K. Chen, H. Ma, L. Che, Z. Li, and B. Wen, "Comparison of meshing characteristics of helical gears with spalling fault using analytical and finite-element methods," *Mech. Syst. Signal Process.*, vol. 121, pp. 279–298, 2019, doi: [10.1016/j.ymssp.2018.11.023](https://doi.org/10.1016/j.ymssp.2018.11.023).

[15] Z. Liu, H. Wei, J. Wei, Z. Xu, and Y. Liu, "Parametric modelling of vibration response for high-speed gear transmission system," *Int. J. Mech. Sci.*, vol. 249, p. 108273, 2023, doi: [10.1016/j.ijmecsci.2023.108273](https://doi.org/10.1016/j.ijmecsci.2023.108273).

[16] F. Choy, Y. Ruan, J. Zakrajsek, F. Oswald, and J. Coy, "Analytical and experimental study of vibrations in a gear transmission," in *27th Joint Propulsion Conference, Sacramento, CA, USA, 24 June 1991 – 26 June 1991*, 1991, pp. 1–20, doi: [10.2514/6.1991-2019](https://doi.org/10.2514/6.1991-2019).

[17] C.I.L. Park, "Transfer matrix of parametric excited system for noise and vibration analyses of helical gear system," *J. Mech. Sci. Technol.*, vol. 35, pp. 4889–4896, 2021, doi: [10.1007/s12206-021-1007-0](https://doi.org/10.1007/s12206-021-1007-0).

[18] C.I.L. Park, "Vibration from a shaft-bearing-plate system due to an axial excitation of helical gears," *J. Mech. Sci. Technol.*, vol. 20, pp. 2105–2114, 2006, doi: [10.1007/BF02916327](https://doi.org/10.1007/BF02916327).

[19] C.I.L. Park, "Characteristics of noise generated by axial excitation of helical gears in shaft-bearing-plate system," *J. Mech. Sci. Technol.*, vol. 29, pp. 1571–1579, 2015, doi: [10.1007/s12206-015-0329-1](https://doi.org/10.1007/s12206-015-0329-1).

[20] Y. Cai and T. Hayashi, "The linear approximated equation of vibration of a pair of spur gears (theory and experiment)," *J. Mech. Des.*, vol. 116, no. 2, pp. 558–564, 1994, doi: [10.1115/1.2919414](https://doi.org/10.1115/1.2919414).

[21] P. Folęga, G. Wojnar, R. Burdzik, and Ł. Konieczny, "Dynamic model of a harmonic drive in a toothed gear transmission system," *J. Vibroeng.*, vol. 16, no. 6, pp. 3096–3104, 2014. [Online]. Available: <https://www.extrica.com/article/15571>

[22] Y. Zeng, J. Zhu, Y. Han, D. Qiu, W. Huang, and M. Xu, "Dynamic modeling and numerical analysis of gear transmission system with localized defects," *Machines*, vol. 13, no. 4, p. 272, 2025, doi: [10.3390/machines13040272](https://doi.org/10.3390/machines13040272).

[23] A.N. Wieczorek, Ł. Konieczny, G. Wojnar, R. Wyroba, K. Filipowicz, and M. Kuczaj, "Reduction of dynamic loads in the drive system of mining scraper conveyors through the use of an innovative highly flexible metal coupling," *Eksplot. Niezawodn. – Maint. Reliab.*, vol. 26, no. 2, pp. 1–17, 2024, doi: [10.17531/ein/181171](https://doi.org/10.17531/ein/181171).

[24] M. Kuczaj, A.N. Wieczorek, Ł. Konieczny, R. Burdzik, G. Wojnar, K. Filipowicz, and G. Gluszek, "Research on vibroactivity of toothed gears with highly flexible metal clutch under variable load conditions," *Sensors*, vol. 23, no. 1, p. 287, 2023, doi: [10.3390/s23010287](https://doi.org/10.3390/s23010287).

[25] G. Wojnar, R. Burdzik, A.N. Wieczorek, and Ł. Konieczny, "Multidimensional data interpretation of vibration signals registered in different locations for system condition monitoring of a three-stage gear transmission operating under difficult conditions," *Sensors*, vol. 21, no. 23, p. 7808, 2021, doi: [10.3390/s21237808](https://doi.org/10.3390/s21237808).

[26] B. Łazarz, G. Wojnar, and P. Czech, "Early fault detection of toothed gear in exploitation conditions (in Polish: Wykrywanie wczesnych faz uszkodzeń kół zębatych w warunkach eksploatacyjnych)," *Eksplot. Niezawodn. – Maint. Reliab.*, vol. 1, no. 49, pp. 68–77, 2011. [Online]. Available: <https://archive.ein.org.pl/2011-01-09>

[27] S. Schmidt, R. Zimroz, and P.S. Heyns, "Enhancing gearbox vibration signals under time-varying operating conditions by combining a whitening procedure and a synchronous processing method," *Mech. Syst. Signal Process.*, vol. 156, p. 107668, 2021, doi: [10.1016/j.ymssp.2021.107668](https://doi.org/10.1016/j.ymssp.2021.107668).

[28] R. Kumar *et al.*, "Fault identification of direct-shift gearbox using variational mode decomposition and convolutional neural network," *Machines*, vol. 12, no. 7, p. 428, 2024, doi: [10.3390/machines12070428](https://doi.org/10.3390/machines12070428).

[29] G. Litak and M.I. Friswell, "Vibration in gear systems," *Chaos Solitons Fractals*, vol. 16, no. 5, pp. 795–800, 2003, doi: [10.1016/S0960-0779\(02\)00452-6](https://doi.org/10.1016/S0960-0779(02)00452-6).

[30] M. Zajíček and J. Dupal, "Analytical solution of spur gear mesh using linear model," *Mech. Mach. Theory*, vol. 118, pp. 154–167, 2017, doi: [10.1016/j.mechmachtheory.2017.08.008](https://doi.org/10.1016/j.mechmachtheory.2017.08.008).

[31] P. Velex and L. Flamand, "Dynamic response of planetary trains to mesh parametric excitations," *J. Mech. Des.*, vol. 118, no. 1, pp. 7–14, 1996, doi: [10.1115/1.2826860](https://doi.org/10.1115/1.2826860).

[32] K. Feng, J.C. Ji, Q. Ni, and M. Beer, "A review of vibration-based gear wear monitoring and prediction techniques," *Mech. Syst. Signal Process.*, vol. 182, p. 109605, 2023, doi: [10.1016/j.ymssp.2022.109605](https://doi.org/10.1016/j.ymssp.2022.109605).

[33] T. Aihara and K. Sakamoto, "Theoretical analysis of nonlinear vibration characteristics of gear pair with shafts," *Theor. Appl. Mech. Lett.*, vol. 12, no. 2, p. 100324, 2022, doi: [10.1016/j.taml.2022.100324](https://doi.org/10.1016/j.taml.2022.100324).

[34] D. Zhang and S. Wang, "Parametric vibration of split gears induced by time-varying mesh stiffness," *Proc. Inst. Mech. Eng., Part C: J. Mech. Eng. Sci.*, vol. 229, no. 1, pp. 18–25, 2014, doi: [10.1177/0954406214531748](https://doi.org/10.1177/0954406214531748).

[35] DynPy, "Github: bogumilchilinski/dynpy," 2025-10-12 current version. [Online]. Available: <https://github.com/bogumilchilinski/dynpy>

[36] B. Chilinski, R. Kwiatkowski, K. Twardoch, and A. Mackoć, "An innovative pendulum-based absorber exploiting time-varying mass dynamics for vibration damping," *Bull. Pol. Acad. Sci. Tech. Sci.*, vol. 73, no. 5, p. e154285, 2025, doi: [10.24425/b-pasts.2025.154285](https://doi.org/10.24425/b-pasts.2025.154285).

[37] K. Twardoch and D. Sierociński, "An analytical approach to gear mesh dynamics for the sustainable design of agricultural machinery drive systems," *Sustainability*, vol. 17, no. 5, p. 1837, 2025, doi: [10.3390/su17051837](https://doi.org/10.3390/su17051837).

[38] K. Twardoch, K. Górska, R. Kwiatkowski, K. Jaśkiewicz, and B. Chilinski, "Adaptive pendulum-tuned mass damper based on adjustable-length cable for skyscraper vibration control," *Sustainability*, vol. 17, no. 14, p. 6301, 2025, doi: [10.3390/su17146301](https://doi.org/10.3390/su17146301).

[39] D. Sierociński, B. Chilinski, F. Gawiński, A. Radomski, and P. Przybyłowicz, "Dynpy–python library for mechanical and electrical engineering: An assessment with coupled electro-mechanical direct current motor model," *Energies*, vol. 18, no. 2, p. 332, 2025, doi: [10.3390/en18020332](https://doi.org/10.3390/en18020332).

[40] M. Żurawski, B. Chilinski, and R. Zalewski, "A novel method for changing the dynamics of slender elements using sponge particles structures," *Materials*, vol. 13, no. 21, p. 4874, 2020, doi: [10.3390/ma13214874](https://doi.org/10.3390/ma13214874).

[41] M. Żurawski, R. Zalewski, and B.D. Chilinski, "Concept of an adaptive-tuned particles impact damper," *J. Theor. Appl. Mech.*, vol. 58, no. 3, pp. 811–816, 2020, doi: [10.15632/jtam-pl/122431](https://doi.org/10.15632/jtam-pl/122431).

[42] "Sympy: 1.12 released," 2023-05-10. [Online]. Available: <https://www.sympy.org/en/index.html>

[43] B. Chilinski, A. Mackoć, and K. Mackoć, "Analytical solution of parametrically induced payload nonlinear pendulation in offshore lifting," *Ocean Eng.*, vol. 259, p. 111835, 2022, doi: [10.1016/j.oceaneng.2022.111835](https://doi.org/10.1016/j.oceaneng.2022.111835).

[44] C.-J. Bahk and R.G. Parker, "Analytical solution for the nonlinear dynamics of planetary gears," *J. Comput. Nonlinear Dyn.*, vol. 6, no. 2, p. 021007, 2011, doi: [10.1115/1.4002392](https://doi.org/10.1115/1.4002392).

[45] "Scipy: 1.15.2 released," 2025-02-16. [Online]. Available: <https://scipy.org>